Drosophila astrocytes cover specific territories of CNS neuropil and are instructed to differentiate by Prospero, a key effector of Notch.

Emilie Peco[1,2], Sejal Davla[1,3], Darius Camp[1.4], Stephanie Stacey[1,3], Matthias Landgraf[5], Don van Meyel[1,2].

[1] Centre for Research in Neuroscience, Department of Neurology and Neurosurgery, McGill University, Montreal, QC, Canada H3G1A4

[2] Research Institute of the McGill University Health Centre, Montreal, QC, Canada H3G1A4

[3] McGill Integrated Program in Neuroscience McGill University, Montreal, QC, Canada H3A2B4

[4] Division of Experimental Medicine, McGill University, Montreal, QC, Canada. H3A1A3

[5] Department of Zoology, University of Cambridge, UK CB2 3EJ

[*]Correspondence:

McGill University Centre for Research in Neuroscience

1650 Cedar Av, L12-401, Montreal, QC, H3G 1A4, Canada

don.vanmeyel@mcgill.ca

Development • Advance article

Abstract

Astrocytes are recognized as critical elements in the formation, fine-tuning, function and plasticity of neural circuits in the central nervous system. However, important questions remain unanswered about the mechanisms instructing astrocyte cell fate. We studied astrogenesis in the ventral nerve cord of Drosophila larvae, where astrocytes have remarkable morphological and molecular similarities to astrocytes in mammals. We reveal the births of larval astrocytes from a multi-glial lineage, their allocation to reproducible positions, and their deployment of ramified arbors to cover specific neuropil territories to form a stereotyped astroglial map. Finally, we unraveled a molecular pathway for astrocyte differentiation in which the Ets protein Pointed and Notch signaling pathway are required for astrogenesis; however, only Notch is sufficient to direct non-astrocytic progenitors toward astrocytic fate. We found that Prospero is a key effector of Notch in this process. Our data identify an instructive astrogenic program that acts as a binary switch to distinguish astrocytes from other glial cells.

Keywords

Introduction

Astrocytes are among the most numerous cells in the mammalian central nervous system (CNS), with protoplasmic astrocytes projecting highly ramified arbors of infiltrative processes among neuronal cell bodies and synapses (Bushong et al., 2004; Distler et al., 1991; Ogata and Kosaka, 2002). Through extensive interactions with neurons, astrocytes employ a host of channels, receptors and transporters to maintain ion and neurotransmitter homeostasis, and modulate and respond to neuronal activity (Clarke and Barres, 2013). Individual astrocytes may coordinate these activities within their micro-anatomical domain since astrocytes occupy exclusive territories with little or no overlap with their neighbors (Bushong et al., 2004; Distler et al., 1991; Halassa et al., 2007; Ogata and Kosaka, 2002). In addition, astrocytes appear tailored for precise roles at region-specific circuitry: within the developing mouse spinal cord, astrocytes are spatially restricted according to their region of origin (Hochstim et al., 2008; Tsai et al., 2012), providing local trophic support for neurons and spatially-encoded information that influences the formation and refinement of neural circuits (Molofsky et al., 2014). Discovering the degree and precision with which astrocytes chart to specific CNS territories is a critical step toward understanding how domain-specific astrocytes locally regulate neural circuit formation and function.

It is well-appreciated that astrocytes emerge from complex interplay between cell-intrinsic programs and extrinsic influences such as secreted or contact-dependent signals from neurons (for reviews see (Kanski et al., 2014; Molofsky et al., 2012)). For example, newborn neurons in mammals stimulate astrogenesis in progenitor cells by secreting the cytokine cardiotrophin-1 (Barnabe-Heider et al., 2005), and by contact-mediated communication via the Notch signaling pathway (Namihira et al.,

2009; Yoon et al., 2008). Notch effectors include the bHLH Hes factors, which inhibit neurogenesis and promote STAT3, a direct activator of astrocytic genes (Kamakura et al., 2004). Another Notch target, the nuclear factor NF1A, is critical for initiating astrogenesis through demethylation of astrocytic gene promoters that can then be bound by STAT3 for transcriptional activation (Deneen et al., 2006). Despite recent progress, defining astrogenic pathways *in vivo* has been complicated by imperfect markers, and because astrocytes in mammals arise from multi-potent progenitors that generate neurons first (Molofsky et al., 2012). For these reasons we investigated astrogenesis *in vivo* by using the *Drosophila* larva CNS, a relatively simple and genetically tractable model. The larval ventral nerve cord (VNC) has a defined number of identifiable glial cells (Beckervordersandforth et al., 2008). This allows the precise positioning and emergence of astrocytes to be followed in exquisite detail, a key advantage compared to mammalian model systems.

Like their mammalian counterparts, *Drosophila* astrocytes extend processes infiltrating the synaptic neuropil, and tile with one another to occupy non-overlapping territories (Awasaki et al., 2008; Doherty et al., 2009; Omoto et al., 2015; Stork et al., 2014). *Drosophila* astrocytes respond to neuronal activity with altered transporter expression and intracellular calcium dynamics (Muthukumar et al., 2014; Stork et al., 2014), they influence CNS synapse number during neural circuit formation (Muthukumar et al., 2014) and modulate locomotor behavior, seizures and olfactory processing (Liu et al., 2014; Rival et al., 2004; Stacey et al., 2010; Stork et al., 2014). However, little is known about how *Drosophila* astrocytes are organized relative to specific regions of the synaptic neuropil, or of the key regulatory programs that govern the acquisition of astrocyte fate versus other glial cell types.

We report that larval astrocytes derive from a lineage that also gives rise to non-astroglial cells. Astrocytes are distinguished by their expression of the homeodomain transcription factor Prospero, known previously for its role in neuroblast lineages to halt stem cell division and initiate neuronal differentiation (Choksi et al., 2006; Vaessin et al., 1991). We find that individual astrocytes are allocated to reproducible regions, and that their infiltrative arbors cover territories of the CNS neuropil that are remarkably stereotyped. Seeking factors essential for the differentiation of astrocytes, we find that Notch signaling is astrogenic, as it is in mammals, and that the Ets transcription factor Pointed is also required. However, only Notch signaling is sufficient to direct non-astrocyte progenitors toward astrocyte fate. We demonstrate that Prospero is a key effector of Notch in this process, identifying the Notch-Prospero program as a critical switch that is both essential and instructive to engage astrocyte differentiation during development.

Results

Longitudinal Glia generate astrocytes, ensheathing and ensheathing/wrapping glia

Longitudinal glia (LG), exclusively derived from the Longitudinal Glioblast (LGB) (Beckervordersandforth et al., 2008; Schmid et al., 1999), are thought to be the embryonic precursors of larval astrocytes, but no systematic high-resolution analysis has mapped their mature identities and organization in first-instar larvae (L1). We resolved this using *AO75-lacZ* (Fig. 1A-B), a specific reporter for embryonic LG (Beckervordersandforth et al., 2008). As in embryos, we found it labeled 9 cell bodies per hemisegment at the interface between neuropil and cortex that were confirmed to be LG by co-labeling with *Nazgul-nGFP*, another LG reporter (Fig. 1A-C") that also happens to be expressed in other glial cells such as cortex glia (Fig. 1B-B', arrows) (Stacey et al., 2010). We then examined subtypes among LG (Fig. 1C-C''', stippled circles) and found that, as in embryos, six of the nine LG express Prospero (Griffiths et al., 2007; Griffiths and Hidalgo, 2004; Ito et al., 1995a). Of the remaining three that did not (Fig. 1C, arrowheads), one expressed *Salm-lacZ* (Fig. 1D-D''', arrowheads) which in embryos marks the lateral posterior-LG (LP-LG) (Beckervordersandforth et al., 2008).

We next assessed LG morphologies using the 'Blown-OUT' technique to visualize small clones of cells. Blown-OUT is akin to the Flp-OUT technique except it employs B3 recombinase instead of Flp to achieve site-specific recombination of a reporter transgene (Nern et al., 2011). Using *Eaat1-Gal4* and *Nazgul-Gal4* (Table 1), clones ranging in size from 1-8 cells were labeled with membrane-targeted RFP (myr−RFP). The only cell found in single-cell clones (Fig. 1G) did not express Prospero (Fig. 1G inset), formed a sheath over the dorsal aspect of the neuropil, and

wrapped a proximal portion of the intersegmental nerve, giving it features of both ensheathing and wrapping glia. Among 2-cell clones, 88% were pairs of Prospero$^+$ astrocytes extending infiltrative processes into the neuropil (Fig. 1E). The remaining 12% of 2-cell clones did not express Prospero (Fig. 1F inset) and were pairs of ensheathing glia enveloping the ventral and medial aspects of the neuropil between neuromeres (Fig. 1F). We confirmed that Prospero was not expressed in ensheathing and ensheathing/wrapping glia labeled with R56C01-Gal4 (Table 1, Fig. 1H). These data confirm that the 9 embryonic LG in each hemisegment become six larval astrocytes (Prospero$^+$), 2 ensheathing glia, and 1 glial cell with combined ensheathing/wrapping features that we deduced to be the LP-LG based on its dorso-medial position (summary in Fig. 1I).

Drosophila astrocytes infiltrate specific neuropil territories

To achieve a better understanding of astrocyte differentiation, the organization of astrocytes must be characterized. Astrocyte cell bodies consistently occupied particular regions around the neuropil (Fig. 1I), comparable to their positions seen in third-instar larval VNC (Ito et al., 1995b; Kato et al., 2011; Stork et al., 2014). Indeed, among the six astrocytes by hemisegment, three astrocytes are at dorsal positions; two are more laterally located whereas one is ventral. More significantly, we discovered that astrocytes in 2-cell clones were non-randomly paired since, based on the relative positions of their cell bodies, 90% could be classified into one of only three categories (Fig. 2A-D). Either both astrocytes in the pair were positioned dorsally (Cat.1 D/D; Fig. 2B), or both astrocytes were positioned laterally (Cat.2 L/L; Fig. 2C) or one dorsal astrocyte was paired with the ventral astrocyte (Cat.3 D/V; Fig. 2D). Since astrocytes in 2-cell clones are likely siblings, non-random pairings indicate that within

each hemisegment there are three sibling-pairs of astrocytes spatially allocated to distinct regions. In order to evaluate how precise their positions were within these regions (dorsal, lateral, ventral), we charted GFP labeled nuclei in 2-cell clones with respect to axon bundles labeled by Fas2 (Fig. 2E-G; (Landgraf et al., 2003b). These provide specific and consistent neuropil landmarks to map astrocytes along the dorso-ventral and medio-lateral axes (Fig. 2F), and the antero-posterior axis (Fig. 2G). Our results indicated that the cell bodies of astrocytes were clearly allocated to one of three distinct regions around the neuropil, yet within each region, their positions were rather imprecise (Fig. 2F-G).

We then asked if regional allocation of astrocyte cell bodies was accompanied by their coverage of specific zones of the neuropil. As in many nervous systems, the *Drosophila* VNC neuropil displays spatial segregation of functionally distinct regions: the dorsal neuropil harbors presynaptic terminals that converge onto motor neurons while the ventral region contains synaptic inputs from sensory neurons (Grueber et al., 2007; Landgraf et al., 2003a; Merritt and Whitington, 1995; Zlatic et al., 2003). We systematically charted the territories covered by astrocyte arbors, mapping 2-cell Blown-OUT clones arbors with respect to their contact with Fas2-axon tracts (Fig. 2E, H-L). When both astrocytes were positioned dorsally (Cat.1 D/D, *n=15*), they consistently infiltrated a dorsal-medial zone that varied only at a single landmark fascicle (Fig. 2I-J; yellow; Cat.1a (*n=9*) vs 1b (*n=6*)). When both astrocytes were positioned laterally (Cat.2 L/L, *n=19*), they covered an invariant lateral territory (Fig. 2I-J; red). Finally, arbors of the dorsal and ventral pair (Cat.3 D/V, *n=20*) infiltrated a ventral-to-medial territory, with variability at one landmark only (Fig. 2I-J; orange; Cat.3a (*n=13*) vs 3b (*n=7*)). Thus, the data reveal a largely stereotyped astroglial map

in which identifiable astrocytes (Fig. 2K) consistently infiltrate specific zones of the synaptic neuropil (Fig. 2J-L).

Lineage mapping and diversification of LG

Reproducibility among astrocytes could stem from stereotyped births and migrations within the lineage. We never observed 2-cell clones pairing an astrocyte and an ensheathing glial cell, suggesting that the last divisions are symmetric. To further understand the lineage we examined *Nazgul-nGFP* with live imaging (Fig. 3A, C). At its onset of expression (0min), four cells per hemisegment were labeled, and could be followed until embryos reached stage 16 (144min). In that time, each of these cells divided only once. These terminal divisions did not appear tightly coordinated or sequential (Fig. 3C). By comparing cell positioning of live cells at stage 16 versus fixed and labeled cells (Fig. 3B), we conclude that the 3 anterior-most progenitors seen at t=0 (red, orange, yellow) give rise to three pairs of Prospero$^+$ astrocytes, while the posterior-most progenitor (cyan) produces the pair of ensheathing glia (Fig. 3D). The idealized view of the LGB lineage we propose in Fig. 3D is supported by over 85% of the 4-cell clones we observed, as 62.9% were composed of the Cat.1D/D and Cat.2L/L pairs of astrocytes, while 22.9% consisted of the Cat.3D/V pair of astrocytes and the ensheathing glia pair. We could not track the origin of the LP-LG, the 9th cell of the LGB lineage, as it became newly-labeled with *Nazgul-nGFP* with no visible progenitor (Fig. 3C, dark blue). Data suggest that LP-LG arises independently within the lineage and might derive from the asymmetric division of the LGB itself (Fig. 3D): i) it was the only LG found in single-cell clones (*n*=13), ii) it was never found in 2-cell clones and iii) none of the few 8-cell clones (*n*=3) we observed included LP-LG.

Astrocytes and ensheathing glia are distinguished by expression of Eaat1 and Eaat2

Astrocytes were shown recently to express the GABA transporter Gat (Stork et al., 2014). Previously, the glutamate recycling enzyme Glutamine synthetase 2, (Thomas and van Meyel, 2007) and the N-β-alanyl-biogenic amine synthetase Ebony (Kato et al., 2011) were shown in Prospero[+] glia. Also, mRNA for Eaat1, the only *Drosophila* glutamate transporter (Besson et al., 2000), and Eaat2, a transporter for taurine and aspartate (Besson et al., 2005; Besson et al., 2011; Besson et al., 2000), were shown to be expressed in discrete subsets of glia in the embryonic CNS (Freeman et al., 2003; Soustelle et al., 2002; Stacey et al., 2010). We raised antisera for Eaat1 and Eaat2, and found that Eaat1 antibody greatly labeled astrocytic membranes (Fig. 4A-A3). Ensheathing glia (Fig. 4, blue brackets) and ensheathing/wrapping glia (Fig. 4, arrows) express lower levels of Eaat1 (Fig. 4A-A3) and, more notably, express Eaat2 (Fig. 4A'-A3'). The latter was confirmed by selective RNAi knock-down of Eaat2 from ensheathing and ensheathing/wrapping glia (Fig. 4C) using the newly characterized *R56C01-Gal4* (Fig. 4E and Table 1). Therefore, subtypes of LG are specialized for the uptake and metabolism of different neuroactive molecules as summarized in Fig. 4D-E.

PointedP1 is required for astrogenesis

What molecular mechanisms promote acquisition of different glial identities? The ETS transcription factor PntP1 is specifically expressed in embryonic LG and required early for their proper differentiation (Klaes et al., 1994). But whether PntP1 selectively contributes to the programs generating the distinct LG subtypes has to be

determined. To examine this, we induced RNAi knock down of *pointed* gene products (i.e. *PntP1* and *PntP2;* (Klambt, 1993)) in all LG using *R25H07*-Gal4 (Fig. 4E and Table 1). At L1, these cells were mis-positioned to only the dorsal perimeter of the neuropil (Fig. 5D), but they retained expression of the glial marker Repo (Fig. S1A-B, G). Remarkably, the analysis of molecular markers to distinguish astrocytes (Prospero, Ebony, Gat, Eaat1^{high}) from ensheathing glia (Eaat2, Eaat1^{low}) revealed specific impairment of astrocyte differentiation. Prospero and Ebony, which are normally co-expressed in astrocytes (Fig. 5A-A'), were lost (Fig. 5D-D'). Also lost were astrocytic processes within the neuropil labeled with a membrane-tethered GFP (Fig. 5E compared to control in Fig. 5B), Eaat1 (Fig. 5F2-F2') or Gat (data not shown). Interestingly, we also observed a broadening of Eaat2-expressing membranes surrounding the neuropil (Fig. 5F1-F2'', brackets) compared to controls (Fig. 5C1-C2''). This suggests that ensheathing glia fate was not impaired by loss of Pointed, and raised the possibility that this led astrocyte to switch to ensheathing glia fate. Similar results were obtained by overexpressing a constitutively active form of the PntP1 antagonist Anterior open (Aop^{ACT}) (Brunner et al., 1994) (Fig.S2, A-D2). Our data reveal that, although all LG need PntP1 for correct positioning, PntP1 is selectively required for the terminal differentiation of astrocytes.

Notch and Prospero promote astrogenesis at the expense of ensheathing glia

The loss of astrocytes caused by the inhibition of Pointed was accompanied by loss of Prospero expression. We showed previously that Notch signaling through Fringe, a glycosyltransferase that sensitizes the Notch receptor to the Delta ligand, maintains expression of Prospero in the anterior-most six LG in stage 16 embryos (Thomas and van Meyel, 2007) and positively regulates *Eaat1* transcripts (Stacey et al., 2010). We

thus asked if Notch might regulate the astrogenic program. To do so, we overexpressed Hairless, a transcriptional repressor of the Notch pathway (Fig. 5G-I2"). In L1 larvae, we found this antagonism of Notch caused severe reduction of Prospero expression but, in contrast to *pnt* RNAi, only modest alteration of cell positioning. Neither cell number nor Repo expression was affected (Fig. S1C and G), but there were severe losses of Ebony (Fig. 5G-G') and, within the neuropil, losses of astrocyte infiltration (CD4-tdGFP+ membranes, Fig. 5H), of Eaat1 (Fig. 5I2-I2') and of Gat (data not shown). We found Eaat1-labeled membranes gathered around the neuropil instead (Fig. 5I2-I2'), accompanied by broadened expression of Eaat2 (Fig. 5I1-I2", brackets). This could result from expansion of ensheathing glia membranes upon loss of astrocytic membranes, or to the transformation of astrocytes into ensheathing glia. To distinguish these two possibilities, we used the Blown-OUT technique to visualize individual cells overexpressing Hairless (Fig. 5N). We found that Prospero-negative Hairless-expressing clones with cell bodies in the positions of dorsal astrocytes adopted an ensheathing-like morphology with membranes at the interface of the neuropil and cortex (compare to control, Fig. 5M), while clones of ensheathing glia were unaffected (data not shown). Altogether, our data indicate that Notch signaling is required for astrocyte differentiation, and that in the absence of Notch cells adopt an ensheathing glia-like profile at both the molecular and morphological levels.

What is the role of Prospero in this process? We found that RNAi knock-down of Prospero itself abolished Ebony expression (Fig. 5J-J') (Kato et al., 2011), and prevented astrocyte infiltration into the neuropil (Fig. 5K-L2'). This was not the result of having fewer cells, since cell number and Repo expression were not affected (Fig. S1D and G). Therefore our results indicate that Prospero is not simply a marker for

developing astrocytes, it is also essential for astrocyte differentiation. On the other hand, Prospero knockdown also broadened expression of Eaat2 along the surface of the neuropil (Fig. 5L1-L2'', brackets). Consistent with this, Blown-OUT clones had flattened appearance and did not infiltrate the neuropil (Fig. 5O). This strongly supports the idea that impairment of astrocyte fate is accompanied by promotion of ensheathing glia fate instead.

Interplay of Pointed, Notch and Prospero in the control of astrogenesis

To assess whether Notch activation could drive ensheathing glia toward an astrocyte fate, we expressed a constitutively active form of Notch (Notch^{ICD}) in LG. Mis-expression of Notch^{ICD} can drive Prospero expression in embryonic LG that do not normally express it (Griffiths and Hidalgo, 2004; Thomas and van Meyel, 2007). Here we found that Notch^{ICD} induced not only ectopic Prospero but also ectopic Ebony (Fig. 6C-C', arrowheads) and Gat (data not shown), and that the domain of Eaat2 expression was severely reduced, especially at medial and ventral neuropil between neuromeres where ensheathing glia normally reside (Fig. 6D2 and D2''). This evidence for an instructive role for Notch signaling in astrogenesis is supported by analysis of Blown-OUT clones expressing Notch^{ICD} (Fig. S3). In controls (n=38), 86.8% were pairs of Prospero-positive astrocytes (Fig. S3A-A') while 13.2% of 2-cell clones were pairs of Prospero-negative ensheathing glia (Fig. S3C-C'). Upon activation of Notch signaling with Notch^{ICD} (n=25), 96% were pairs of Pros+ astrocytes (Fig. S3B-D') and 4% were pairs of ensheathing glia − in these cases, the ensheathing glia did not express Prospero (Fig. S3D-D', white arrowhead). Among astrocyte clones, the increase largely comes in the Cat.3 D/V (13.2% in controls vs 28% in Notch^{ICD}). Similarly, in 4-cell Blown-OUT clones where in controls (n=28)

46.4% were comprised of the Cat.3 D/V astrocyte pair and 2 ensheathing glia, upon Notch^{ICD} expression all clones were astrocytes only. Together, these results indicate that Notch induces astrocyte differentiation at the expense of ensheathing glia. When Notch^{ICD} did not convert ensheathing glia to astrocytes, the ensheathing glia did not express Prospero (Fig. S3D, white arrowhead) signifying that Prospero might be a key effector of Notch in this process. In keeping with this, we found Prospero knock down entirely mitigated the ability of Notch^{ICD} to induce ectopic astrogenesis (Fig. 6E-F2).

Thus, both PntP1 and Notch signaling are required for Prospero expression and differentiation of astrocytes, and Notch signaling is sufficient to induce Prospero and drive astrogenesis in cells that would otherwise become ensheathing glia (Fig. 6C-D2"). We wondered if Notch^{ICD} could induce Prospero in this manner if PntP1 function were blocked by its antagonist Aop. In these conditions, animals were unable to hatch, and so were examined at stage 17 of embryogenesis (Fig. 6G-H2). We found that Notch^{ICD} could not induce Prospero or Ebony (Fig. 6G-G') or infiltration of the neuropil (Fig. 6H2). Therefore *pointed* blockade renders LG incapable of becoming astrocytes in response to Notch. Since overexpression of PntP1 does not induce ectopic Prospero expression (data not shown), our data argues that the early role of PntP1 in the differentiation of LG allows Notch signaling to selectively induce Prospero in the subset that are fated to become astrocytes (Fig. 6I).

Prospero itself drives astrocyte differentiation

Others have shown that Prospero can activate glial gene expression (Choksi et al., 2006; Kato et al., 2011), and our data here suggested that Prospero might play an active role in instructing astrocytic fate. We mis-expressed Prospero specifically in Prospero-negative LG using *R56F03-Gal4* (Fig. 4E and Table 1). Remarkably, mis-

expression of Prospero in these cells led to their ectopic expression of the astrocyte markers Ebony (Fig. 7C2-C3 arrowheads) and Gat (data not shown) compared to control (fig. 7A1-A3), and caused these cells to grow Eaat1-positive astrocyte-like processes into the neuropil (Fig. 7C1-C1' and D4 compared to control Fig. 7A1-A1', B4). This pro-astrocytic effect was accompanied by the loss of Eaat2 expression in all cells that normally express it (Fig. 7D4' versus control Fig. 7B4'). Based on this, we conclude that Prospero is both necessary and sufficient for astrogenesis.

Discussion

We report the differentiation of *Drosophila* astrocytes from a multipotent glioblast that also gives rise to ensheathing glia. We provide new insight into the organization of the synaptic neuropil by discovering that *Drosophila* astrocytes are allocated to specific regions and cover stereotyped territories to form an astroglial map. In addition, we describe a program for astrocyte differentiation in which PntP1 allows Notch signaling to engage its key effector Prospero.

Allocation of larval astrocytes, and formation of a precise astroglial map

We have shown that *Drosophila* astrocytes are reliably allocated to consistent regions, as seen for mammalian astrocytes (Hochstim et al., 2008; Tsai et al., 2012). Molecular heterogeneity among astrocytes could account for their distinct positioning but currently we have no evidence for it. Within these regions, astrocyte cell bodies appear imprecisely positioned and yet, to a surprising degree, their infiltrative arbors chart very precisely to particular regions of the neuropil. This specific topography of the 3 pairs of astrocytes delineate an astroglial map whose means of assembly are currently unknown. It seems predisposed by soma position, and is surely influenced by FGF-mediated arbor ingrowth (Stork et al., 2014) and tiling, yet because soma positioning is imprecise and FGF ligands are produced broadly within the neuropil, these cannot entirely account for such precise coverage. Future research will be needed to investigate additional mechanisms that could contribute to astroglial map formation, such as targeting of astrocyte arbors via local guidance cues, or tiling of neighboring astrocytes via mutual exclusion.

In mammals, astrocytes organize into exclusive spatial domains with limited overlap with neighbors, and this topography plays a role in the function of neural

networks (Lopez-Hidalgo and Schummers, 2014). In light of this it is intriguing that the dorsal region of *Drosophila* VNC neuropil harbors synaptic inputs onto motor neurons and the ventral region contains synaptic inputs from sensory neurons (Grueber et al., 2007; Landgraf et al., 2003a; Merritt and Whitington, 1995; Zlatic et al., 2003). Thus, coverage of discrete territories by specific astrocytes could partition synapses in motor versus sensory neuropil, or perhaps into other functionally important subdivisions. During development, this might provide local spatial information to aid the maturation and refinement of neural circuits, and in the mature CNS this could create functionally isolated islands to provide localized balance and coordination of ions and neurotransmitters (Halassa et al., 2007).

Astrocyte generation from a multipotent glioblast requires Pointed, Notch, and Prospero

Previously, division of the LGB was shown to be followed by the medial migration of its two daughter cells to positions just dorsal to the nascent longitudinal axon tracts (Jacobs et al., 1989). Here, we provide evidence that one daughter cell gives rise to three sibling pairs of astrocytes and one pair of ensheathing glia. The other daughter cell is likely to give rise to the ensheathing/wrapping glial cell known as LP-LG in embryos. This is notably different from the adult *Drosophila* brain where astrocytes and ensheathing glia emerge from distinct post-embryonic lineages (Awasaki et al., 2008), indicating several modes of generating astrocytes in *Drosophila*.

We identified three key factors for astrocyte differentiation also sufficient to switch the developmental fate of LG: the Ets protein PntP1, Notch signaling, and the homeoprotein Prospero. Our data support the idea that PntP1 has an early role in the differentiation of all LG (Klaes et al., 1994) and, through a mechanism currently

unknown, it allows productive Notch signaling to selectively instruct progenitors toward the astrocyte fate. Whether this astrogenic role for Ets family factors is conserved among species remains to be explored but it is noteworthy that glial defects in *Drosophila pointed* mutants can be rescued with vertebrate Ets-1 (Albagli et al., 1996), and that Ets-1 regulates the formation of radial glia in *Xenopus* (Kiyota et al., 2007).

We showed that in the absence of Notch signaling glial progenitors that should become astrocytes generate ensheathing glia instead. Conversely, Notch activation instructs cells that normally become ensheathing glia to acquire the morphology and molecular profile of astrocytes. These alternative glial fates are not due to the well-characterized role of Notch in asymmetric cell divisions, since astrocytes and ensheathing glia are born coincidentally from symmetric terminal divisions (Fig. 3). Instead, we propose they arise from Notch-dependent neuron-to-glial communication during embryogenesis. We previously found that Fringe sensitizes Notch to stimulation from developing axons bearing Delta, thus maintaining Prospero and *Eaat1* expression in a subset of LG (Stacey et al., 2010; Thomas and van Meyel, 2007). Knowing now that Prospero$^+$ cells develop into astrocytes, these data support the idea that astrogenesis is promoted by neuron-to-glial Notch signaling. Astrogenesis in response to neuron-to-glial Notch signaling is likely conserved in mammals, where intermediate neuronal progenitors and newly-born neurons express Delta-like 1 (Castro et al., 2006; Namihira et al., 2009) and its obligate cofactor Mindbomb1 (Yoon et al., 2008). These have been shown, although *in vitro*, to activate Notch signaling in radial glia and confer astroglial potential on them (Namihira et al., 2009). Still, Notch in this context is permissive rather than instructive, as Notch-

activated progenitors will only differentiate into astrocytes if they subsequently receive stimulation from gliogenic cytokines (Namihira et al., 2009).

Remarkably, we found that Prospero is a key effector of the astrogenic effect of Notch. Prospero expression is selectively maintained in newly-born and mature astrocytes. Prospero is required for the differentiation of astrocytes, but not of ensheathing glia, despite their common lineage. Indeed, Prospero misexpression alone transforms ensheathing glia into astrocytes, based on a number of molecular and morphological criteria. Together, these data suggest that Prospero acts as a binary switch to distinguish astrocytes from other glial cells. Prospero orthologs exist in nematodes and mammals, and in mice they have been shown to be important for the development of a variety of organs and cell types including neurons (Elsir et al., 2012). In vertebrates, Prospero-related homeobox 1 (Prox1) is expressed in astrocyte-like Müller cells of the retina of adult mammals and fish (Cid et al., 2010) and other glial cells (Lavado and Oliver, 2007), but whether it is involved in glial differentiation remains unknown. Interestingly, *Drosophila* glia expressing Prospero and Ebony have been shown to regenerate in response to stab injury in the larval VNC (Kato et al., 2011). Knowing now that these cells are astrocytes adds an intriguing item to the list of functions that *Drosophila* astrocytes share with their mammalian counterparts. Indeed, our discoveries here into how *Drosophila* astrocytes are born, how they infiltrate specific zones of the CNS neuropil, and how they differentiate in response to a specific astrogenic program will undoubtedly strengthen their utility as model system to study fundamental aspects of astrocyte biology and astrocyte-neuron interactions.

Materials and methods

Fly stocks and genetics

Drosophila melanogaster stocks were obtained from Bloomington Stock Center (*UAS-Prospero, UAS-PointedP1, UAS-aop.ACT, P{PZ}salm^{03602}, UAS-RNAi^{TRIP} for PntP1* (*HMS01452*), *UAS-CD4-tdGFP, P{GMR25H07-Gal4}, P{GMR56C01-Gal4}* and *P{GMR56F03-Gal4}*); the Vienna *Drosophila* Resource Center (*UAS-RNAi* for Prospero (transformant ID 101477) and Eaat2 (transformant ID 104371)); published sources (*UAS-Notch^{ICD}*; *UAS-Hairless*; *Eaat1-Gal4*; *AO75-lacZ;*, *20XUAS-B3RT>dSTOP-B3RT>myr::RFP*). We previously reported *CG31235-nGFP* and *CG31235*-Gal4, here renamed *Nazgul-nGFP* and *Nazgul-Gal4*, and null mutants for *Eaat1* (*Eaat1$^{SM2/SM2}$*) (Stacey et al., 2010).

For all RNAi experiments, control animals carried a Gal4 driver and a fluorescent reporter (i.e. *UAS-nls-GFP*). For experimental groups, we added a single copy of the RNAi construct.

Immunohistochemistry and imaging

Late embryos and L1 larvae were dissected and prepared as described previously (Stacey et al., 2010), but for anti-Eaat1 and anti-Eaat2, tissues were treated with Bouin's fixative (Polysciences Inc.) for 10 minutes at room temperature. Developmental Studies Hybridoma Bank monoclonal antibodies were mouse anti-Prospero (MR1A, 1:100), mouse anti-Discs-large (Dlg) (4F3, 1:200), mouse anti-Repo (8D12, 1:10), and mouse anti–Fasciclin2 (Fas2) (1D4,1:200). Other antibodies were: anti-β-galactosidase (β-gal) (1:1000, MP Biomedicals #0855976), anti-Nazgul

(1:500) (von Hilchen et al., 2010), anti-DsRed (1:1000, Clontech #632496), anti-Ebony (1:500), anti-Gat (1:2000) (Stork et al., 2014), anti-Eaat1 (1:5000) and anti-Eaat2 (1:5000). Goat secondary antibodies were from Molecular Probes: Alexa Fluor 647 anti-rabbit (#A21244) and anti-mouse (#A21235) and from Jackson Immunoresearch Dylight594 anti-rabbit (#115-517-003), Rhodamine Red-X anti-mouse (#115-295-146) or anti-rabbit (#111-295-144), and anti-guinea pig Alexa Fluor 647 (#106-605-003) or DyLight549 (#106-506-003). Samples were mounted in SlowFade Gold reagent (Molecular Probes). Fluorescence images were acquired with an Olympus Fluoview FV1000/BX-63 confocal laser scanning microscope, and processed using Fiji and Imaris (Bitplane). 3D reconstructions were generated with Fiji's 3D Viewer plug-in.

To quantify GFP+/Repo+ cells, the total number within 4 adjacent abdominal segments (from among A1-A7) was divided by 4, for each of 5 animals for every genotype.

Generation of Blown-OUT clones

Dr. Tzumin Lee generously provided an unpublished stock carrying heat shock-inducible B3 recombinase (*hs-B3*) at attP18. Virgin *hs-B3* females were crossed to males that were either *w⁻;Eaat1-Gal4,UAS-nls-GFP;20XUAS-B3RT>dSTOP-B3RT>myr::RFP (attP2)*, or *Nazgul-Gal4,UAS-nGFP;20XUAS-B3RT>dSTOP-B3RT>myr::RFP(attP2)*. Mating adults were moved to grape juice-agar plates for 12h at 25°C, and L1 larvae were selected 0–2 h post-hatching and raised on fresh plates at 25°C until analyzed 12h afterward. No heat-shock was applied as there was sufficient B3 expression to generate clones. For Blown-OUT clones expressing Hairless, Prospero RNAi or Notch[ICD], males *20XUAS-B3RT>dSTOP-*

B3RT>myr::RFP(attP40);R25H07-Gal4,UAS-nGFP were crossed to virgin females that were either *hsB3;UAS-Hairless*, *hsB3;UAS-ProsperoRNAi* or *hsB3;;UAS-Notch^{ICD}*. For better efficiency of GAL4-UAS, grape plates containing mating adults were maintained at 29°C till analyzed.

Live Imaging

Nazgul-nGFP embryos were collected for 3h and aged for 5h at 25°C, dechorionated manually, positioned on a Gas Permeable Slide Plate (Coy Lab Products) with ventral side up, mounted in halocarbon oil 27 (Sigma) under a coverslip and imaged on a Olympus Fluoview FV1000/BX-63 confocal microscope every 8 minutes using dry 20X objective from stage 13 to 16.

Charting astrocytes and their territories

The positions of astrocytes around the neuropil were mapped relative to reference landmarks stained with anti-Fas2 (Landgraf et al., 2003b). On each axis, the distance between these reference landmarks was normalized to 1, and then the nucleus of each astrocyte was plotted in relation to that distance. Landmarks for the dorsal-ventral axis were the fascicles D_i and V_L. For the medial-lateral axis they were the CNS midline and fascicle D_L. For the anterior-posterior axis they were the transverse projection 1 (TP1) in adjacent segments. To chart the territories covered by astrocytes within the CNS neuropil, we catalogued their contacts with each one of seven identifiable Fas2-fascicles.

Eaat1 and Eaat2 antibody production

Sequences encoding the extracellular loop of Eaat1 (aa117-195 of Eaat1-PA) or Eaat2 (aa131-226 of Eaat2-PA) were cloned into pGEX to produce N-terminal GST fusion proteins IPTG-inducible (0.2mM) in BL21 cells (Invitrogen). GST-Eaat1 and GST-Eaat2 were purified with standard procedures for insoluble proteins (Rebay and Fehon, 2009). Purified GST-Eaat1 (1ug/ul) was injected into rabbits and GST-Eaat2 (0.5ul/ul) into guinea pigs. Sera were tested by immunolabeling on dissected CNS tissues from control animals, null mutants for *Eaat1,* and RNAi knock-down for *Eaat2*.

Acknowledgements

Competing Interests Statement

The authors declare no competing financial interests.

Author contributions

E.P., M.L. and D.J.vM. conceived the study; E.P., S.D. and S.M.S performed experiments; E.P, S.D., D.C. and D.J.vM. analyzed the data; E.P. and D.J.vM. wrote the manuscript; all authors approved the manuscript.

Funding

References

Albagli, O., Klaes, A., Ferreira, E., Leprince, D. and Klambt, C. (1996). Function of ets genes is conserved between vertebrates and Drosophila. *Mechanisms of development* **59**, 29-40.

Awasaki, T., Lai, S. L., Ito, K. and Lee, T. (2008). Organization and postembryonic development of glial cells in the adult central brain of Drosophila. *The Journal of neuroscience : the official journal of the Society for Neuroscience* **28**, 13742-13753.

Barnabe-Heider, F., Wasylnka, J. A., Fernandes, K. J., Porsche, C., Sendtner, M., Kaplan, D. R. and Miller, F. D. (2005). Evidence that embryonic neurons regulate the onset of cortical gliogenesis via cardiotrophin-1. *Neuron* **48**, 253-265.

Beckervordersandforth, R. M., Rickert, C., Altenhein, B. and Technau, G. M. (2008). Subtypes of glial cells in the Drosophila embryonic ventral nerve cord as related to lineage and gene expression. *Mechanisms of development* **125**, 542-557.

Besson, M. T., Re, D. B., Moulin, M. and Birman, S. (2005). High affinity transport of taurine by the Drosophila aspartate transporter dEAAT2. *J Biol Chem* **280**, 6621-6626.

Besson, M. T., Sinakevitch, I., Melon, C., Iché-Torres, M. and Birman, S. (2011). Involvement of the drosophila taurine/aspartate transporter dEAAT2 in selective olfactory and gustatory perceptions. *J Comp Neurol* **519**, 2734-2757.

Besson, M. T., Soustelle, L. and Birman, S. (2000). Selective high-affinity transport of aspartate by a Drosophila homologue of the excitatory amino-acid transporters. *Curr Biol* **10**, 207-210.

Brunner, D., Ducker, K., Oellers, N., Hafen, E., Scholz, H. and Klambt, C. (1994). The ETS domain protein pointed-P2 is a target of MAP kinase in the sevenless signal transduction pathway. *Nature* **370**, 386-389.

Bushong, E. A., Martone, M. E. and Ellisman, M. H. (2004). Maturation of astrocyte morphology and the establishment of astrocyte domains during postnatal hippocampal development. *Int J Dev Neurosci* **22**, 73-86.

Castro, D. S., Skowronska-Krawczyk, D., Armant, O., Donaldson, I. J., Parras, C., Hunt, C., Critchley, J. A., Nguyen, L., Gossler, A., Gottgens, B., et al. (2006). Proneural bHLH and Brn proteins coregulate a neurogenic program through cooperative binding to a conserved DNA motif. *Developmental cell* **11**, 831-844.

Choksi, S. P., Southall, T. D., Bossing, T., Edoff, K., de Wit, E., Fischer, B. E., van Steensel, B., Micklem, G. and Brand, A. H. (2006). Prospero acts as a binary switch between self-renewal and differentiation in Drosophila neural stem cells. *Developmental cell* **11**, 775-789.

Cid, E., Santos-Ledo, A., Parrilla-Monge, M., Lillo, C., Arevalo, R., Lara, J. M., Aijon, J. and Velasco, A. (2010). Prox1 expression in rod precursors and Muller cells. *Experimental eye research* **90**, 267-276.

Clarke, L. E. and Barres, B. A. (2013). Emerging roles of astrocytes in neural circuit development. *Nature reviews. Neuroscience* **14**, 311-321.

Deneen, B., Ho, R., Lukaszewicz, A., Hochstim, C. J., Gronostajski, R. M. and Anderson, D. J. (2006). The transcription factor NFIA controls the onset of gliogenesis in the developing spinal cord. *Neuron* **52**, 953-968.

Distler, C., Dreher, Z. and Stone, J. (1991). Contact spacing among astrocytes in the central nervous system: an hypothesis of their structural role. *Glia* **4**, 484-494.

Doherty, J., Logan, M. A., Tasdemir, O. E. and Freeman, M. R. (2009). Ensheathing glia function as phagocytes in the adult Drosophila brain. *The Journal of neuroscience : the official journal of the Society for Neuroscience* **29**, 4768-4781.

Elsir, T., Smits, A., Lindstrom, M. S. and Nister, M. (2012). Transcription factor PROX1: its role in development and cancer. *Cancer metastasis reviews* **31**, 793-805.

Freeman, M. R., Delrow, J., Kim, J., Johnson, E. and Doe, C. Q. (2003). Unwrapping glial biology: Gcm target genes regulating glial development, diversification, and function. *Neuron* **38**, 567-580.

Griffiths, R. C., Benito-Sipos, J., Fenton, J. C., Torroja, L. and Hidalgo, L. (2007). Two distinct mechanisms segregate Prospero in the longitudinal glia underlying the timing of interactions with axons. *Neuron Glia Biol* **3**, 75-88.

Griffiths, R. L. and Hidalgo, A. (2004). Prospero maintains the mitotic potential of glial precursors enabling them to respond to neurons. *Embo J* **23**, 2440-2450.

Grueber, W. B., Ye, B., Yang, C. H., Younger, S., Borden, K., Jan, L. Y. and Jan, Y. N. (2007). Projections of Drosophila multidendritic neurons in the central nervous system: links with peripheral dendrite morphology. *Development* **134**, 55-64.

Halassa, M. M., Fellin, T., Takano, H., Dong, J. H. and Haydon, P. G. (2007). Synaptic islands defined by the territory of a single astrocyte. *The Journal of*

neuroscience : the official journal of the Society for Neuroscience **27**, 6473-6477.

Hochstim, C., Deneen, B., Lukaszewicz, A., Zhou, Q. and Anderson, D. J. (2008). Identification of positionally distinct astrocyte subtypes whose identities are specified by a homeodomain code. *Cell* **133**, 510-522.

Ito, K., Urban, J. and Technau, G. M. (1995a). Distribution, Classification, and Development of Drosophila Glial-Cells in the Late Embryonic and Early Larval Ventral Nerve Cord. *Roux Arch Dev Biol* **204**, 284-307.

---- (1995b). Distribution, classification, and development of Drosophila glial cells in the late embryonic and early larval ventral nerve cord. *Roux's Arch Dev Biol* **204**, 284-307.

Jacobs, J. R., Hiromi, Y., Patel, N. H. and Goodman, C. S. (1989). Lineage, migration, and morphogenesis of longitudinal glia in the Drosophila CNS as revealed by a molecular lineage marker. *Neuron* **2**, 1625-1631.

Jenett, A., Rubin, G. M., Ngo, T. T., Shepherd, D., Murphy, C., Dionne, H., Pfeiffer, B. D., Cavallaro, A., Hall, D., Jeter, J., et al. (2012). A GAL4-driver line resource for Drosophila neurobiology. *Cell Rep* **2**, 991-1001.

Kamakura, S., Oishi, K., Yoshimatsu, T., Nakafuku, M., Masuyama, N. and Gotoh, Y. (2004). Hes binding to STAT3 mediates crosstalk between Notch and JAK-STAT signalling. *Nature cell biology* **6**, 547-554.

Kanski, R., van Strien, M. E., van Tijn, P. and Hol, E. M. (2014). A star is born: new insights into the mechanism of astrogenesis. *Cell Mol Life Sci* **71**, 433-447.

Kato, K., Forero, M. G., Fenton, J. C. and Hidalgo, A. (2011). The glial regenerative response to central nervous system injury is enabled by pros-notch and pros-NFkappaB feedback. *PLoS Biol* **9**, e1001133.

Kiyota, T., Kato, A. and Kato, Y. (2007). Ets-1 regulates radial glia formation during vertebrate embryogenesis. *Organogenesis* **3**, 93-101.

Klaes, A., Menne, T., Stollewerk, A., Scholz, H. and Klämbt, C. (1994). The ETS transcription factors encoded by the Drosophila gene pointed direct glial cell differentiation in the embryonic CNS. *Cell* **78**, 149-160.

Klambt, C. (1993). The *Drosophila* gene *pointed* encodes two ETS-like proteins which are involved in the development of the midline glial cells. *Development* **117**, 163-176.

Landgraf, M., Jeffrey, V., Fujioka, M., Jaynes, J. B. and Bate, M. (2003a). Embryonic origins of a motor system: motor dendrites form a myotopic map in Drosophila. *PLoS Biol* **1**, E41.

Landgraf, M., Sanchez-Soriano, N., Technau, G. M., Urban, J. and Prokop, A. (2003b). Charting the Drosophila neuropile: a strategy for the standardised characterisation of genetically amenable neurites. *Developmental biology* **260**, 207-225.

Lavado, A. and Oliver, G. (2007). Prox1 expression patterns in the developing and adult murine brain. *Developmental dynamics : an official publication of the American Association of Anatomists* **236**, 518-524.

Liu, H., Zhou, B., Yan, W., Lei, Z., Zhao, X., Zhang, K. and Guo, A. (2014). Astrocyte-like glial cells physiologically regulate olfactory processing through the modification of ORN-PN synaptic strength in Drosophila. *Eur J Neurosci* **40**, 2744-2754.

Lopez-Hidalgo, M. and Schummers, J. (2014). Cortical maps: a role for astrocytes? *Curr Opin Neurobiol* **24**, 176-189.

Merritt, D. J. and Whitington, P. M. (1995). Central projections of sensory neurons in the Drosophila embryo correlate with sensory modality, soma position, and proneural gene function. *The Journal of neuroscience : the official journal of the Society for Neuroscience* **15**, 1755-1767.

Molofsky, A. V., Kelley, K. W., Tsai, H. H., Redmond, S. A., Chang, S. M., Madireddy, L., Chan, J. R., Baranzini, S. E., Ullian, E. M. and Rowitch, D. H. (2014). Astrocyte-encoded positional cues maintain sensorimotor circuit integrity. *Nature* **509**, 189-194.

Molofsky, A. V., Krencik, R., Ullian, E. M., Tsai, H. H., Deneen, B., Richardson, W. D., Barres, B. A. and Rowitch, D. H. (2012). Astrocytes and disease: a neurodevelopmental perspective. *Genes Dev* **26**, 891-907.

Muthukumar, A. K., Stork, T. and Freeman, M. R. (2014). Activity-dependent regulation of astrocyte GAT levels during synaptogenesis. *Nat Neurosci* **17**, 1340-1350.

Namihira, M., Kohyama, J., Semi, K., Sanosaka, T., Deneen, B., Taga, T. and Nakashima, K. (2009). Committed neuronal precursors confer astrocytic potential on residual neural precursor cells. *Developmental cell* **16**, 245-255.

Nern, A., Pfeiffer, B. D., Svoboda, K. and Rubin, G. M. (2011). Multiple new site-specific recombinases for use in manipulating animal genomes. *Proc Natl Acad Sci U S A* **108**, 14198-14203.

Ogata, K. and Kosaka, T. (2002). Structural and quantitative analysis of astrocytes in the mouse hippocampus. *Neuroscience* **113**, 221-233.

Omoto, J. J., Yogi, P. and Hartenstein, V. (2015). Origin and development of neuropil glia of the Drosophila larval and adult brain: Two distinct glial populations derived from separate progenitors. *Developmental biology* **404**, 2-20.

Rebay, I. and Fehon, R. G. (2009). Preparation of insoluble GST fusion proteins. *Cold Spring Harbor protocols* **2009**.

Rival, T., Soustelle, L., Cattaert, D., Strambi, C., Iche, M. and Birman, S. (2006). Physiological requirement for the glutamate transporter dEAAT1 at the adult Drosophila neuromuscular junction. *J Neurobiol* **66**, 1061-1074.

Rival, T., Soustelle, L., Strambi, C., Besson, M. T., Iche, M. and Birman, S. (2004). Decreasing glutamate buffering capacity triggers oxidative stress and neuropil degeneration in the Drosophila brain. *Curr Biol* **14**, 599-605.

Schmid, A., Chiba, A. and Doe, C. Q. (1999). Clonal analysis of Drosophila embryonic neuroblasts: neural cell types, axon projections and muscle targets. *Development* **126**, 4653-4689.

Soustelle, L., Besson, M. T., Rival, T. and Birman, S. (2002). Terminal glial differentiation involves regulated expression of the excitatory amino acid transporters in the Drosophila embryonic CNS. *Developmental biology* **248**, 294-306.

Stacey, S. M., Muraro, N. I., Peco, E., Labbe, A., Thomas, G. B., Baines, R. A. and van Meyel, D. J. (2010). Drosophila glial glutamate transporter Eaat1 is regulated by fringe-mediated notch signaling and is essential for larval locomotion. *The Journal of neuroscience : the official journal of the Society for Neuroscience* **30**, 14446-14457.

Stork, T., Sheehan, A., Tasdemir-Yilmaz, O. E. and Freeman, M. R. (2014). Neuron-glia interactions through the Heartless FGF receptor signaling pathway mediate morphogenesis of Drosophila astrocytes. *Neuron* **83**, 388-403.

Thomas, G. B. and van Meyel, D. J. (2007). The glycosyltransferase Fringe promotes Delta-Notch signaling between neurons and glia, and is required for subtype-specific glial gene expression. *Development* **134**, 591-600.

Tsai, H. H., Li, H., Fuentealba, L. C., Molofsky, A. V., Taveira-Marques, R., Zhuang, H., Tenney, A., Murnen, A. T., Fancy, S. P., Merkle, F., et al. (2012). Regional astrocyte allocation regulates CNS synaptogenesis and repair. *Science* **337**, 358-362.

Vaessin, H., Grell, E., Wolff, E., Bier, E., Jan, L. Y. and Jan, Y. N. (1991). prospero is expressed in neuronal precursors and encodes a nuclear protein that is involved in the control of axonal outgrowth in Drosophila. *Cell* **67**, 941-953.

von Hilchen, C. M., Hein, I., Technau, G. M. and Altenhein, B. (2010). Netrins guide migration of distinct glial cells in the Drosophila embryo. *Development* **137**, 1251-1262.

Yoon, K. J., Koo, B. K., Im, S. K., Jeong, H. W., Ghim, J., Kwon, M. C., Moon, J. S., Miyata, T. and Kong, Y. Y. (2008). Mind bomb 1-expressing intermediate progenitors generate notch signaling to maintain radial glial cells. *Neuron* **58**, 519-531.

Zlatic, M., Landgraf, M. and Bate, M. (2003). Genetic specification of axonal arbors: atonal regulates robo3 to position terminal branches in the Drosophila nervous system. *Neuron* **37**, 41-51.

Table 1. Gal4 drivers used in this study.

Gal4 driver expression characterized in LG by us (*Nazgul-, R25H07-, R56C01-,* and *R56F03-Gal4*) or others as indicated (*Eaat1-Gal4*). These lines also have expression in other cells, but are specified here only for M-ISNG.

Gal4 drivers	Expression in		Onset of GFP detection in LG [a]	References
	Longitudinal Glia	M-ISNG		
Eaat1-Gal4	All (Weaker in Pros-negative cells)	weak	Stage 11	(Beckervordersandforth et al., 2008; Rival et al., 2006; Rival et al., 2004; Stacey et al., 2010)
Nazgul-Gal4	All	yes	Stage 12-13	(Stacey et al., 2010); this work
R25H07-Gal4	All	stochastic	Stage 13	(Jenett et al., 2012); this work
R56C01-Gal4	Ensheathing glia Ensheathing/wrapping glia	yes	Late stage 17	
R56F03-Gal4	Ensheathing glia Ensheathing/wrapping glia (stochastic expression in rare astrocytes)	yes	Stage 14	

[a] In this work Gal4 lines were crossed to UAS-GFP, and dechorionated embryos were live-mounted in halocarbon oil to be assessed for GFP expression with confocal microscopy.
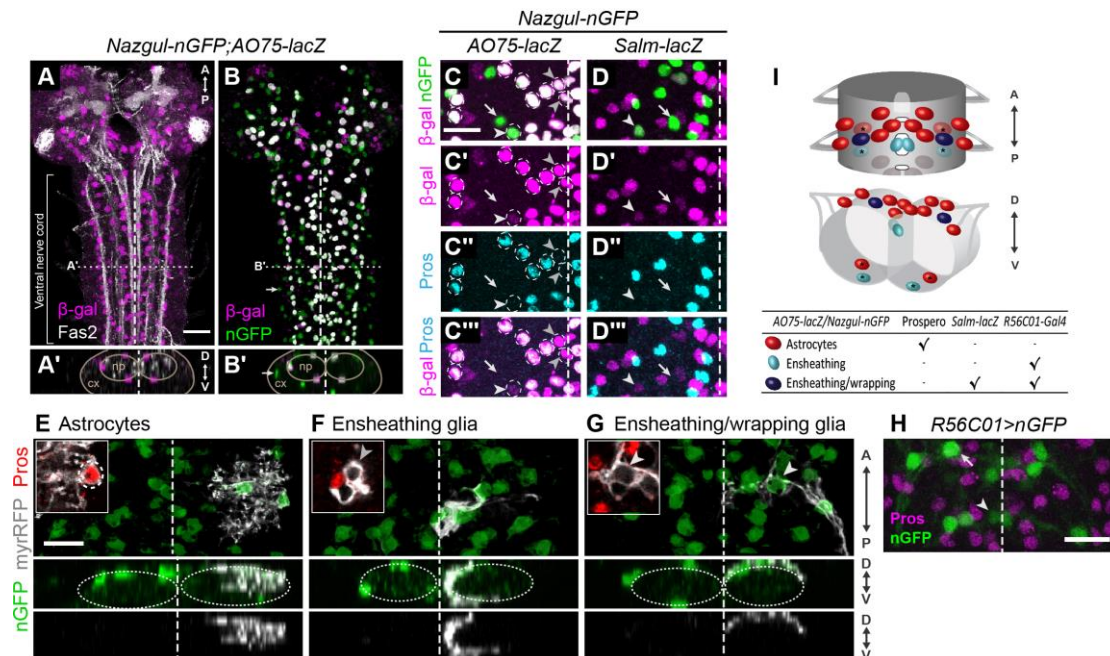
Figures

Figure 1. Astrocytes, ensheathing glia and ensheathing/wrapping glia derive from LG

(A-B') L1 larvae LG labeled with *AO75-lacZ* (magenta) and (A-A') axon tracts with Fas2 (white) or (B-B') *Nazgul-nGFP* (green) which labels LG and other glia (i.e. cortex glia, arrows). All *AO75-lacZ* co-express *Nazgul-nGFP*. 3D horizontal views of confocal Z-stack (A-B), transverse sections (A'-B'). Neuropil (np), cortex (cx).

(C-C''') Among 9 LG by hemisegment (AO75-lacZ+, stippled circles), 6 LG express Pros (cyan). Arrowheads, Pros-negative LG. (D-D''') LP-LG expresses *Salm-lacZ* (arrowheads). C-D, arrows show M-ISNG (*Nazgul-nGFP+* but not *AO75-lacZ*).

(E-G) Blown-OUT clones reveal LG morphologies. LG nuclei labeled with *nGFP* (green), and clones with *myr-RFP* (white) driven by *Eaat1-Gal4* (E-G). 2-cell clones of 2 astrocytes infiltrating the neuropil (E), or 2 ensheathing glia enveloping the medial and ventral neuropil (F). Single-cell clones were ensheathing/wrapping glia,

covering the dorsal neuropil and the proximal part of the intersegmental nerve (G). Only astrocytes express Prospero (insets). Images are horizontal 3D reconstructions (top) or orthogonal views (bottoms).

(H) Non-astrocytic LG do not express Prospero. *R56C01-Gal4;UAS-nGFP* was used to specifically label ensheathing (arrowhead) and ensheathing/wrapping glia (arrow) (Table 1). Prospero (magenta) shows no overlap with nGFP (green). Horizontal view; maximal projection of confocal Z-stack.

(I) Idealized larval VNC neuropil (one segment). Each hemisegment has 6 astrocytes, 2 ensheathing glia and 1 ensheathing/wrapping glia.

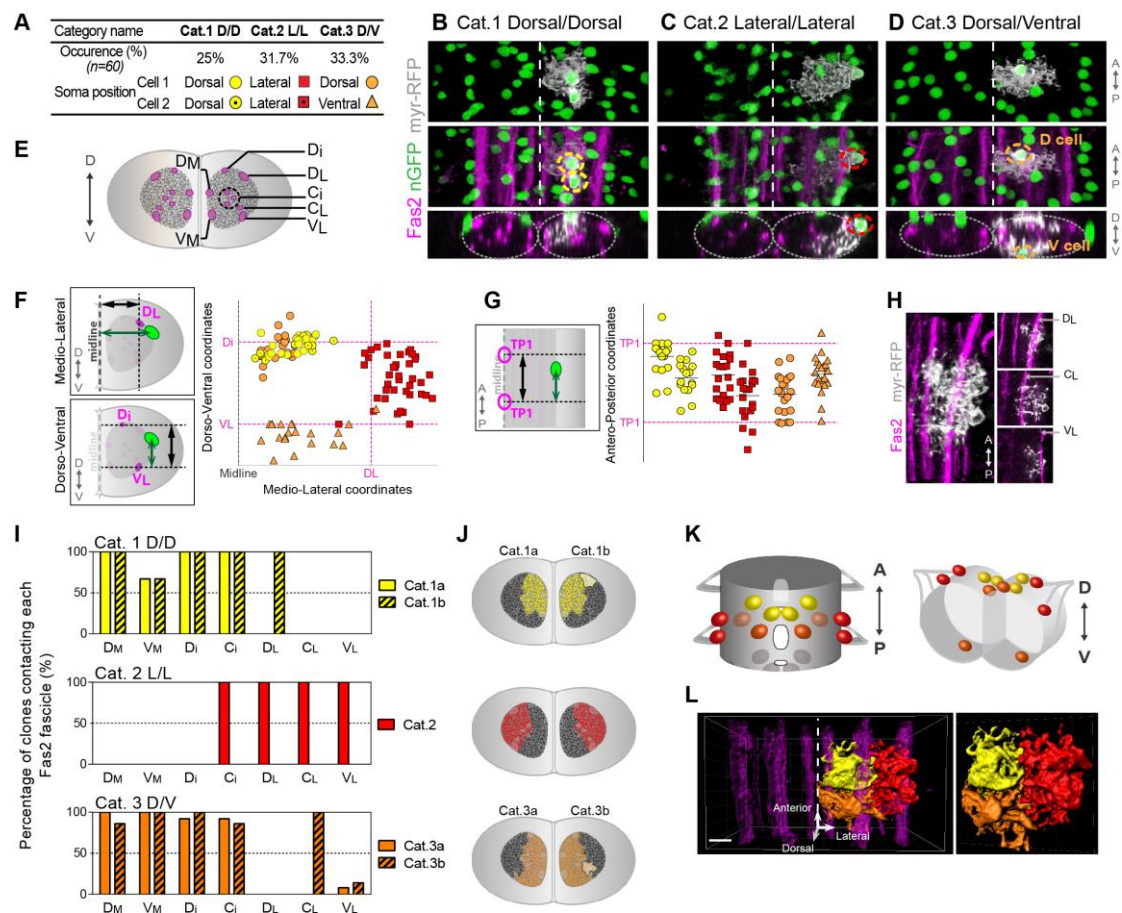Dashed line, midline. Scale bars, 20 µm (A-B') and 10 µm for others.

Figure 2. Astrocytes cover stereotyped territories of the CNS neuropil.

(A-G) Astrocyte cell bodies allocate to particular regions around the synaptic neuropil.

(A-D) 3 categories of astrocyte 2-cell Blown-OUT clones obtained with Eaat1-Gal4 driver. (A) Classification summary. (B) Both astrocytes dorsal to the neuropil (Cat.1 D/D), (C) both astrocytes lateral (Cat.2 L/L), or (D) one dorsal and one ventral (Cat.3 D/V). Glial nuclei labeled with nGFP (green), clones with myr-RFP (white) and axon tracts with anti-Fas2 (magenta). Stippled circles point to astrocyte nuclei within clones. 3D reconstructions of Z-stacks, anterior up. At bottom are transverse sections, dorsal up. Dashed line, midline. Scale bars, 10 μm.

(E-G) Within each region, astrocyte positions are rather imprecise. (E) Schematic of larval VNC cross section with major Fas2-axon bundles (magenta) used to chart 2-cell

astrocyte clones, named according to their dorso-ventral (<u>D</u>orsal, <u>C</u>entral, <u>V</u>entral) and medio-lateral (<u>M</u>edial, <u>I</u>ntermedial, <u>L</u>ateral) position.

(F-G) Relative coordinates of each astrocyte nucleus. Charting along (F) medio-lateral and dorso-ventral axes with reference to the midline and specific Fas2-axon bundles or (G) antero-posterior axis using the Fas2 positive transverse projection 1 (TP1). In diagrams at left, black arrows, reference distance between landmarks; green arrows, distance from nGFP-labeled nucleus to landmark.

(H-L) Astrocytes reproducibly cover distinct neuropil territories. (H) Technique for charting astrocyte territories: example of a 2-cell clone whose arbor (myr-RFP, white) contacts specific Fas2-axon bundles (magenta). Left, 3D reconstruction of Z-stack; right, single-Z sections at levels in the neuropil. Anterior up.

(I) Contacts made by astrocytes with Fas2 axon bundles in each category of 2-cell clones. Results expressed as the percentage of clones from a given category that contacted indicated fascicles. Cat.2 L/L territories are invariant ($n=19$), while Cat.1 D/D ($n=15$) and Cat.3 D/V ($n=20$) exhibit modest variability by which they can be subdivided further.

(J) Transverse views of 2D astroglial maps illustrating our findings (C) on how astrocytes parcel the neuropil territory (dorsal is up).

(K) Idealized spatial placement of each sibling-pair of astrocytes cell bodies in a segment.

(L) 3D reconstruction model (Imaris) of 6 astrocytes in a hemisegment, composite of 3 distinct 2-cell clones. Right panel, enlarged view. Dashed line, midline. Scale bar, 30 µm.
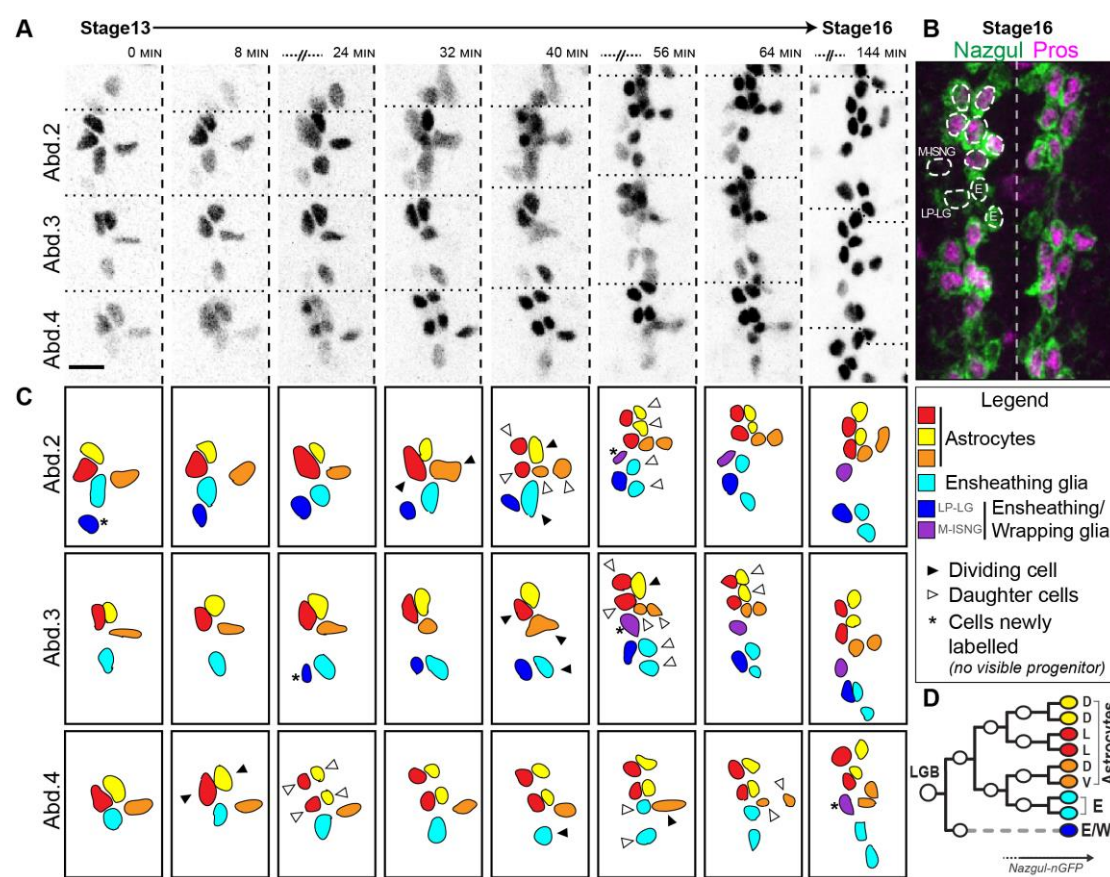
Figure 3. Live imaging of the births of astrocytes and ensheathing glia.

(A) LG visualized with *Nazgul-nGFP* , embryonic stages 13 to 16. Horizontal views of 3 abdominal hemisegments (Abd.2-4). Anterior up; dashed vertical lines, midline. Time is shown in minutes (MIN) with images at selected time points.

(B) Stage 16 embryo fixed VNC: Nazgul (green) labels 9 LG and M-ISNG; Prospero (magenta) co-labels in astrocytes.

(C) Schematic of A. At 0 and 8 min, 4 cells consistently arranged in each hemisegment and by 64 min had divided only once (black arrowheads). Through their reproducible positioning at 144 min the mature identities of the resulting 8 cells were assigned based on cell arrangement in B. Astrocytes are in yellow (Cat.1 D/D), red (Cat.2 L/L) or orange (Cat.3 D/V) and ensheathing glia in cyan. *Nazgul-nGFP* also

newly-labeled 1 or 2 additional cells in each hemisegment (asterisks), corresponding to ensheathing/wrapping glia LP-LG (blue) and M-ISNG (purple).

(D) Idealized view of LGB lineage. LGB is giving rise to 3 pairs of astrocytes, 1 pair of ensheathing glia (E) and a single ensheathing/wrapping glial cell (E/W).
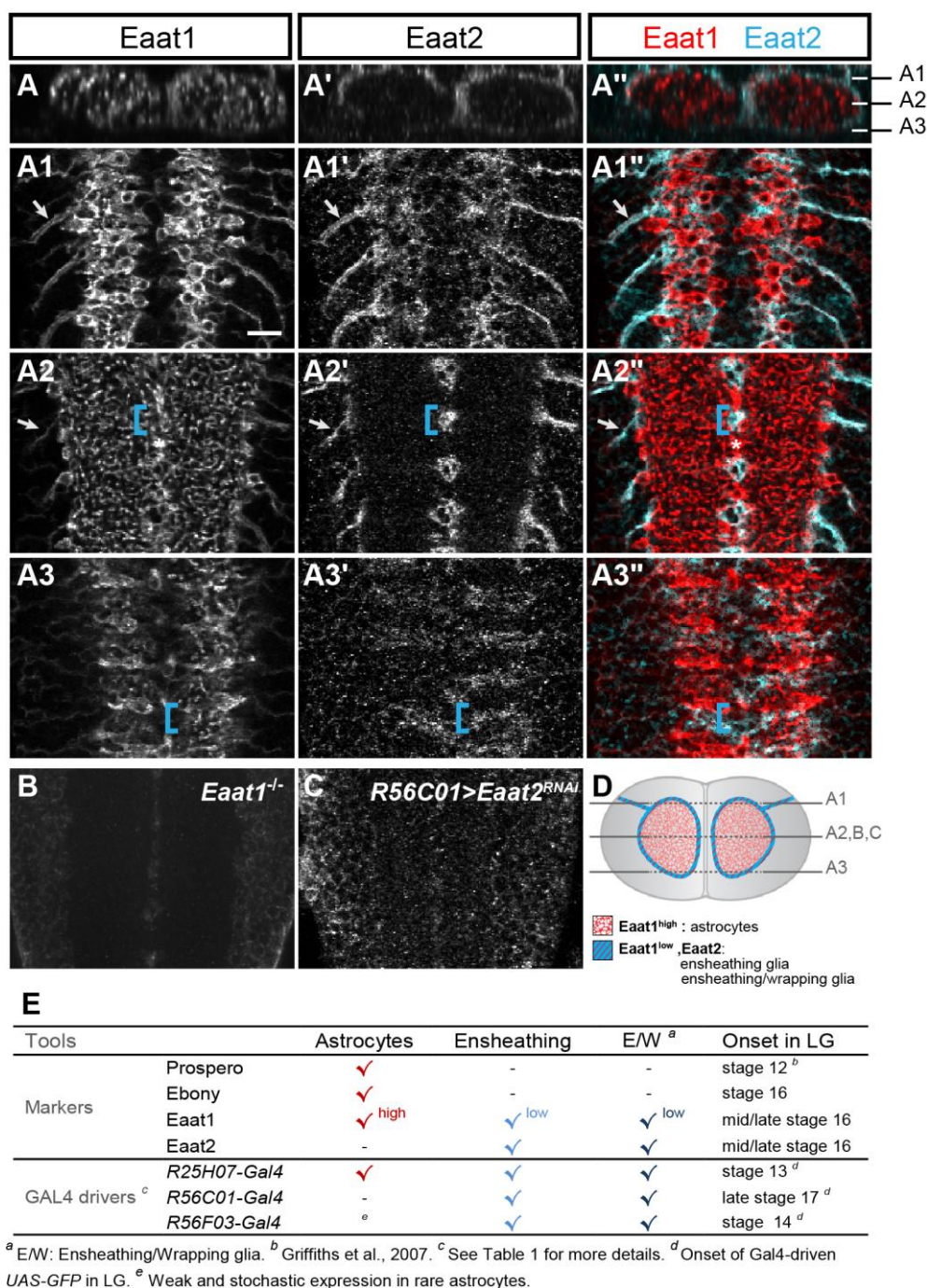
Figure 4. Eaat1 and Eaat2 expression distinguish LG subtypes.

(A-A3''') Co-labeling for the glutamate transporter Eaat1 and the taurine/aspartate transporter Eaat2 in L1 VNC. (A-A'') Transverse images noting the focal planes of the horizontal images (A1-A3; single Z-sections). (A-A3) Eaat1 is expressed at high levels on astrocytic membranes, at lower levels in ensheathing glia and

ensheathing/wrapping glia LP-LG (blue brackets) and M-ISNG (arrows), and by midline glia (asterisks). (A'-A3') Eaat2 is restricted to ensheathing glia covering the medial and ventral neuropil between neuromeres (blue brackets) and ensheathing/wrapping glia (arrows).

(B) Specificity of Eaat1 antiserum confirmed by loss of Eaat1 immunoreactivity in *Eaat1* null mutants.

(C) Specificity of Eaat2 antiserum confirmed by Eaat2 RNAi knockdown with *R56C01-Gal4,* a driver specific to ensheathing and ensheathing/wrapping glia.

(D) Schematic to illustrate the findings.

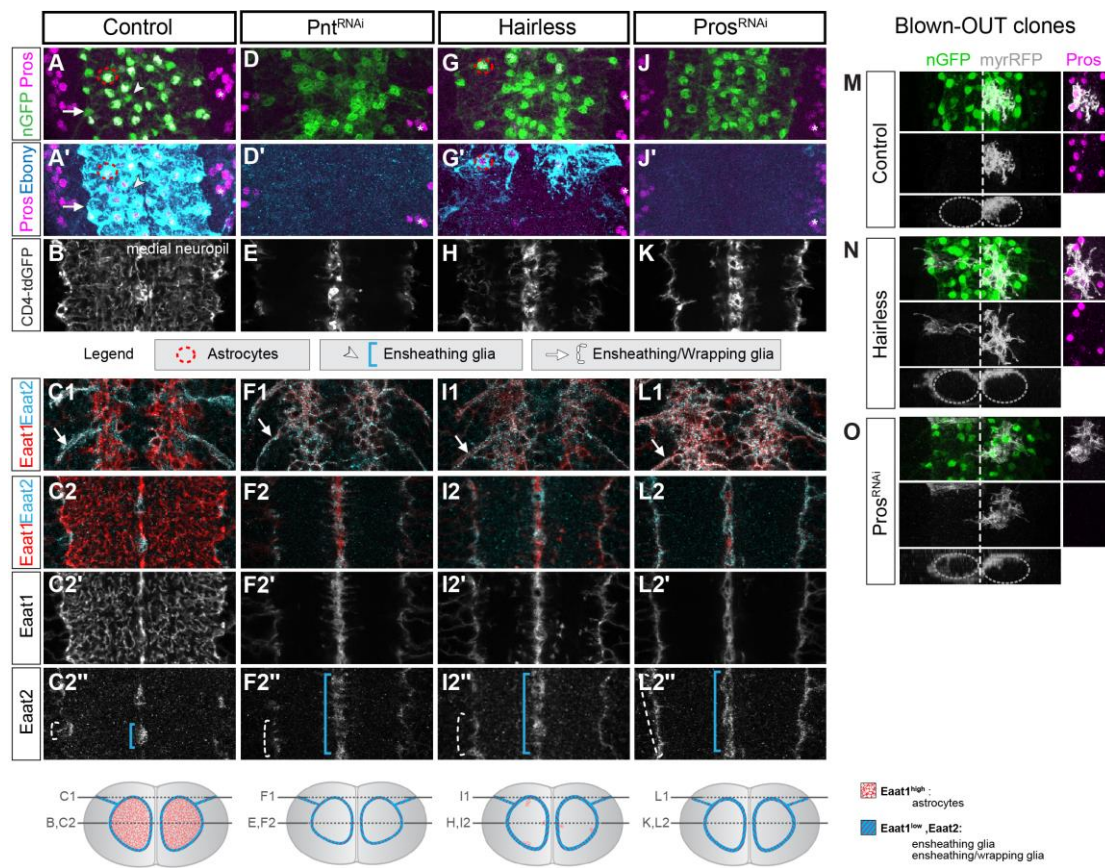(E) Key molecular markers (antibodies) and Gal4-drivers used in this study.

Figure 5. Astrogenesis requires Pointed, Notch and Prospero.

Representative images of L1 VNCs double-labeled for (A-A')-(J-J') Prospero and Ebony, or (C1-C2'')-(L1-L2'') Eaat1 and Eaat2. (A-A')-(J-J') are maximum projection of confocal Z-stacks; other panels are single Z-section at focal planes shown at bottom. *R25H07-Gal4* was used to target all LG. Legend applies to all panels. Bottom schematics illustrate findings shown in (C1-C2'')-(L1-L2''). Scale bar, 10 μm.

(A-C2'') A typical example of control (*n*=15). *n* represents the number of VNCs examined.

(D-F2'') Pointed RNAi (*n*=12). Prospero and Ebony expression are lost and LG mispositioned (D-D'), astrocytic processes marked by the expression of a membrane-tethered GFP (CD4-tdGFP) shown at medial level in the neuropil (E) or Eaat1 (F2-

F2'), fail to infiltrate the neuropil; Eaat2 expression broadens (F2'',brackets), and co-expression of Eaat1 and Eaat2 increases (F1).

(G-I2'') Inhibition of Notch with Hairless (*n*=10). Loss of Prospero and Ebony in most GFP+ LG (G-G'). Astrocytic processes marked by CD4-tdGFP (H) or Eaat1 (I2-I2') seldom infiltrate the neuropil, Eaat2 labeling broadens (brackets, I2''), and co-expression of Eaat1 and Eaat2 expands (I1).

(J-L2'') Prospero RNAi has effects similar to Hairless (*n*=10).

(M-O) Blown-OUT analysis of Notch inhibition and Prospero RNAi knockdown. *Nazgul-Gal4* was used to label glial cell nuclei with GFP (green), 2-cell Blown-OUT clones with myr-RFP (white), and astrocytes with Prospero (magenta, right column). All panels are horizontal sections (anterior is up), but bottom panel that are transverse views (dorsal is up). Dashed lines indicate the midline; dotted ovals outline the neuropil. (M) Control 2-cell astrocyte clone (Cat.1 D/D): both cells infiltrate the neuropil and express Prospero. (N) Notch inhibition with Hairless: two pairs of 2-cell clones in the positions of astrocytes fail to infiltrate the neuropil and do not express Prospero. (O) Prospero RNAi knockdown has effects similar to Hairless: loss of Prospero, lack of neuropil infiltration.
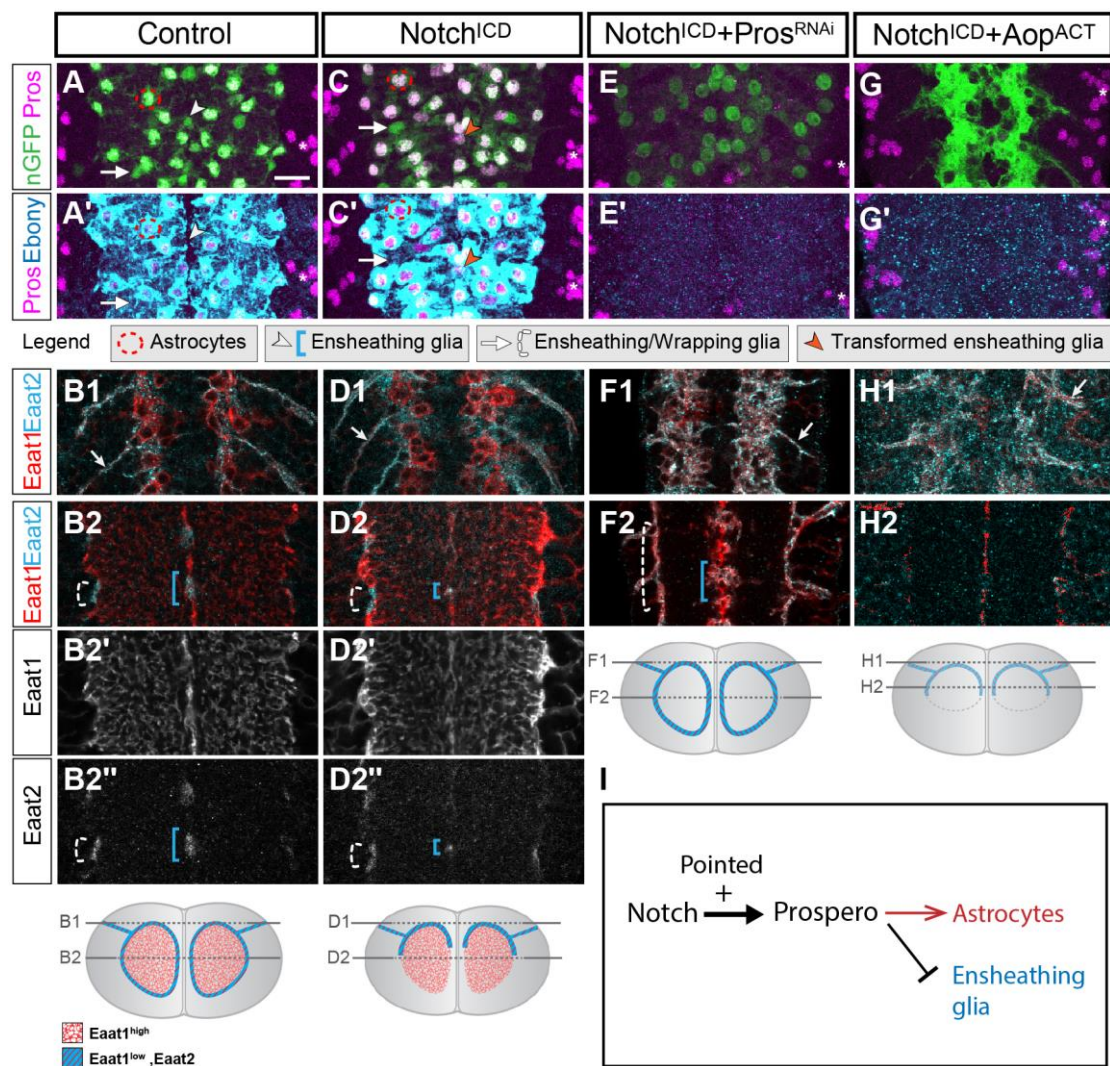
Figure 6. Notch induction of astrogenesis requires Prospero and PntP1.

L1 larval (A-F2) or E17 (G-H2) VNCs co-labeled for (A-A')-(G-G') Prospero and Ebony (maximum projection of Z-stack), or (B1-B2")-(H1-H2) Eaat1 and Eaat2 (single Z-section at focal planes shown at bottom). *R25H07-Gal4,UAS-nGFP* used to target all LG. Legend applies to all panels. Schematics at bottom illustrate the findings of (B1-B2")-(H1-H2). Scale bar, 10 μm.

(A-B2") Control (*n*=15).

(C-D2") Activation of Notch signaling with Notch^{ICD} (*n*=12). Ensheathing glia are induced to express Prospero and Ebony (arrowheads in C-C'), and lose expression of

Eaat2 (blue bracket in D2). Ensheathing/wrapping glia are not sensitive to Notch activation, as they do not express ectopic Prospero or Ebony (arrows in C-C') and Eaat2 remains unaffected (arrow in D1, stippled white brackets in D2-D2").

(E-F2) Simultaneous knockdown of Prospero (n=12) blocks the astrogenic effects of Notch signaling (Ebony expression, membrane infiltration) on ensheathing glia.

(G-H2) Notch activation does not overcome the effect of PntP1 inhibition with Aop^{ACT}(n=10). Additional controls at embryo stage 17 found in Fig. S2.

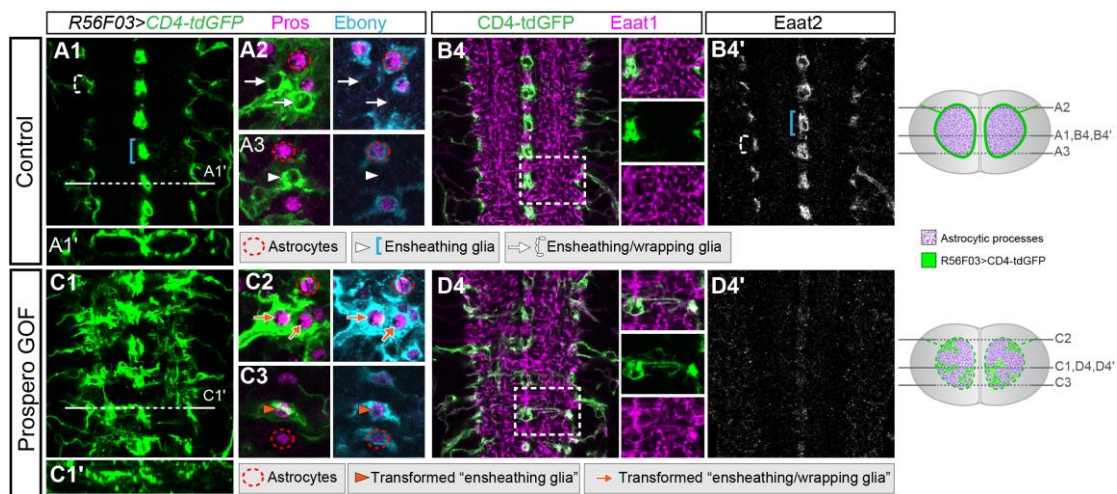(I) Interplay of Pointed, Notch and Prospero.

Figure 7. Prospero is sufficient to transform ensheathing glia into astrocytes.

Single horizontal Z-sections; A1' and C1' are transverse views at levels indicated by dashed lines in A1 and C1. Schematics summarize the findings and note the focal planes of indicated panels.

(A1-B4') Control (*n*=15). *R56F03-Gal4* was used to drive *UAS-CD4-tdGFP* (green) to target ensheathing glia (cell bodies ventral, A3 and C3; arrowheads) and ensheathing/wrapping glia (cell bodies dorsal, A2 and C2; arrows). These cells lie flat around the neuropil (A1-A1';B4), and do not express the astrocyte markers Prospero (magenta) or Ebony (cyan) (arrowheads). Yet, they express Eaat2 (B4').

(C1-D4') Prospero misexpression (Prospero GOF; *n*=25) makes ensheathing glia and ensheathing/wrapping glia adopt astrocyte-like features: they express Ebony (cyan; C2, C3), their processes infiltrate the neuropil (C1-C1'; D4), and they lose Eaat2 expression (D4').